Effect of Surface Modification on Uptake Rates of Isobutane in MFI Crystals: An Infrared Microscopy Study

Christian Chmelik,*[,†] Arati Varma,[†] Lars Heinke,[†] Dhananjai B. Shah,[†,‡] Jörg Kärger,[†] Friedrich Kremer,[†] Ursula Wilczok,[§] and Wolfgang Schmidt[§]

Faculty of Physics and Earth Sciences, University of Leipzig, Linnéstrasse 5, 04103 Leipzig, Germany; Department of Chemical & Biomedical Engineering, Cleveland State University, 2121 Euclid Avenue Cleveland, Ohio 44115; and Max Planck Institute for Coal Science, D-45470 Mülheim, Germany

Received June 19, 2007. Revised Manuscript Received September 12, 2007

Many recent investigations have confirmed the presence of surface barriers in a variety of zeolites. These surface barriers can have a significant effect on the overall rates of mass transfer and have the potential to significantly reduce the effectiveness of zeolites in industrial applications. In this study, the strength of the surface barrier was manipulated in a well-defined way and correlated with the rate of isobutane uptake. Silicalite-1 crystals were synthesized and were surface treated with trimethyl-, triethyl- and tripropylchlorosilanes. It was hypothesized that with the increasing size of the alkyl group the pore windows would be increasingly blocked, thereby effectively decreasing the pore size and increasing the surface barriers. The rates of adsorption and desorption of isobutane in untreated and treated samples were monitored by infrared microscopy. For differential pressure steps, adsorption and desorption responses were mirror images of one another. For large pressure steps, the rate of adsorption was much higher than that of desorption, indicating a significant variation of intracrystalline diffusivity with loading. The adsorption/desorption curves were analyzed considering (1) the presence of only intracrystalline diffusion and (2) surface barrier followed by intracrystalline diffusion. The measured rates of adsorption/desorption were significantly lower for the surface treated samples when compared with those for the untreated samples. Moreover, the strength of the surface resistance increased with the size of the alkyl group in chlorosilanes used for surface treatment.

Introduction

Molecular sieves are crystalline aluminosilicates with a well-defined, uniform, and molecular-sized pore system.[1] They have found numerous applications in industry in the areas of adsorptive separations and catalytic reactions.[2,3] Many of these applications exploit the interplay between the sizes of the diffusing adsorbate molecules vis-à-vis the size of the pore window. Separation of linear and branched hydrocarbons with 5A molecular sieves is a classic example of sieving separation processes wherein the linear hydrocarbons with a smaller critical diameter are able to diffuse through the window size of 4.3 Å and access the internal cavity while the branched hydrocarbons with a larger kinetic diameter are blocked out and thus separated. Kinetic separation based on differing rates of diffusion through the pores has also been used to separate two components as is the case in the separation of nitrogen and oxygen with carbon molecular sieves. By changing the effective diameter of the pore, one may effectively change the relative rates of diffusion and hence enhance the performance of molecular sieves for a particular application. The use of cation exchange to increase or decrease the effective window size in A-type zeolite is well-known.[2] Recently, it has been demonstrated that by changing the dehydration temperature for titanosilicate molecular sieves one can effectively change the size of the pore opening to accomplish size-selective adsorption of molecules.[4]

Another possible way of changing the overall rates of mass transfer in zeolites is to manipulate the strength of surface resistance. Presence of surface barrier/resistance has been found in many of our recent single crystal investigations using interference microscopy (IFM). Diffusion of methanol in large crystals of ferrierite has been studied with IFM, and the results indicated the presence of surface resistance in this system.[5] Recent studies of desorption of isobutane from ZSM-5 crystals by IFM[6,7] have evidently shown the presence of significant surface resistance as indicated by the pronounced concentration decrease near the edge of the crystal.

* Corresponding author: Tel +49 341 9732531; Fax +49 341 9732549; e-mail chmelik@physik.uni-leipzig.de.
[†] University of Leipzig.
[‡] Cleveland State University.
[§] Max Planck Institute for Coal Science.

(1) Barrer, R. M. *Zeolites and Clay Minerals as Sorbents and Molecular Sieves*; Academic Press: London, 1978.
(2) Ruthven, D. M. *Principles of Adsorption and Adsorption Processes*; Wiley & Sons: New York, 1984.
(3) Ruthven, D. M.; Farooq, S.; Knaebel, K. S. *Pressure Swing Adsorption*; VCH: New York, 1994.
(4) Kuznicki, S. M.; Bell, V. A.; Nair, S.; Hillhouse, H. W.; Jacubinas, R. M.; Braunbarth, C. M.; Toby, B. H.; Tsapatsis, M. *Nature (London)* **2001**, *412*, 720.
(5) Kortunov, P.; Chmelik, C.; Kärger, J.; Rakoczy, R. A.; Ruthven, D. M.; Traa, Y.; Vasenkov, S.; Weitkamp, J. *Adsorption* **2005**, *11*, 235.
(6) Chmelik, C.; Kortunov, P.; Vasenkov, S.; Kärger, J. *Adsorption* **2005**, *11*, 455.
(7) Kortunov, P.; Vasenkov, S.; Chmelik, C.; Karger, J.; Ruthven, D. M.; Wloch, J. *Chem. Mater.* **2004**, *16*, 3552.

10.1021/cm071632o CCC: $37.00
Published on Web 11/08/2007

Experimentally measured internal concentration profiles of methanol in CrAPO-5 clearly showed the existence of a significant surface resistance.[8] Results obtained from interference microscopy studies strongly suggest that surface barriers probably exist in many zeolites.

The nature of such surface barriers is not clear. They may arise from either complete blockage of some pores on the surface or partial blockage of all surface pores. Irrespective of the nature of the barrier, its relevance and its impact on zeolite performance cannot be overemphasized. Such barriers, in many cases, effectively lower the overall rates of mass transfer and hence affect the zeolite performance negatively. Therefore, it is important to investigate the nature of surface barriers and their effect on the overall rate of mass transfer. However, in order to do this, one must be able to produce/eliminate surface barriers and change their strengths in a consistent manner.

Surface modification may be one way to introduce surface barriers. Wloch[9] subjected ZSM-5 crystals to hydrofluoric acid treatment to etch the surface and reduce the strength of the surface barrier or completely remove it. The uptake rates of *n*-hexane in HF-treated crystals were measured gravimetrically and were found to be significantly higher than those for the untreated crystals. Similar studies of diffusion of isobutane in these etched and nonetched ZSM-5 crystals have also been performed,[7] but the uptake was monitored by IFM. It was shown that the surface resistance could be successfully reduced by HF treatment. However, it was not completely eliminated.

Surface silanization has also been used quite extensively to modify the surface of ZSM-5 zeolites and alter their shape selective properties.[10–14] Chemical vapor or liquid deposition of alkoxysilanes such as tetraethoxysilane (TEOS) or tetramethoxysilane (TMOS) on ZSM-5 is the preferred method of accomplishing surface modification. Since the kinetic diameter of these molecules is larger than the ZSM-5 pore diameter, the hydroxyl groups at or near the surface of the zeolite react with TEOS or TMOS molecules to form Si–O–Si or Si–O–Al bonds. Also, an inert silica layer is deposited on the outside surface or near the pore mouth region, thereby effectively reducing the effective pore opening and increasing the surface resistance. Intracrystalline diffusivity of cyclohexane in ZSM-5 for both treated and untreated crystals has been measured by zero length chromatography.[12] The results were interpreted in terms of pore mouth blockage. On the other hand, the frequency response technique has been used to measure diffusion of toluene in surface-modified HZSM-5, and results were interpreted in terms of increased tortuosity resulting from surface modification.[15] Recently, two novel ways of changing the surface resistance have been reported in the literature. The surface resistance of zeolite L was manipulated by selective modification of channel entrances with triethoxysilated coumarin.[16] Another approach to change the surface resistance was by insertion of a stopcock molecule into the channels of zeolite L followed by its functionalization.[17]

In spite of these several initiatives to study the effect of surface modification on the intracrystalline diffusivities in zeolites, no systematic study has been performed on producing surface barriers of differing strengths and correlating their strengths with the overall rates of diffusion. In the present study, we have looked into this aspect. We have used silanization to modify the silicalite-1 surface and introduce surface barriers in a measured way. Three different chlorosilanes with trimethyl, triethyl, and tripropyl groups ($(CH_3)_3SiCl$, $(C_2H_5)_3SiCl$, $(C_3H_7)_3SiCl$) have been used for surface treatment with the objective of producing surface barriers of increasing strengths. The rates of adsorption/desorption of isobutane in untreated and treated silicalite-1 crystals have been measured with IR microscopy (IRM) to correlate the rate of mass transfer with the strength of the surface barriers.

Experimental Section

Method. The application of FTIR (Fourier transform infrared) and micro-FTIR spectroscopy for investigating molecular transport in zeolites was spearheaded by the pioneering work of Karge and co-workers.[18–20] The FTIR microscopy setup used in the present investigation comprised an IR-Microscope UMA 500 (Bio-Rad) equipped with a FTIR FTS 6000 spectrometer (Figure 1a) and a vacuum system. The measurements by FTIR microscopy were performed as follows. Several crystals were introduced into an optical cell (Figure 1b) and were activated as described later. First, the microscope was switched to the optical mode, which allowed the choice of a particular zeolite crystal for the measurements and masking it by a rectangular aperture of about $100 \times 220\ \mu m^2$ in the plane of the crystal image (Figure 1c). A smaller aperture size, in principle, would allow spatially resolved measurements of different crystal parts. However, the signal measured from the whole crystal was sufficient for this study. Then the microscope was switched to the IR-transmittance mode. In this mode, the intracrystalline FTIR absorbance spectra of the crystal masked by the aperture were recorded (Figure 1d). The spectra were recorded before and after loading of the crystal from the gas phase with isobutane. The absorbance spectra obtained by dividing and taking logarithms of the transmittance spectra before and after loading the crystal were used for data analysis.

The integrals under characteristic absorbance bands of the guest molecules in these spectra were assumed to be proportional to the integrals of the local concentration in the direction of the IR beam.

(8) Lehmann, E.; Vasenkov, S.; Kärger, J.; Zadrozna, G.; Kornatowski, J.; Weiss, Ö.; Schüth, F. *J. Phys. Chem. B* **2003**, *107*, 4685.
(9) Wloch, J. *Microporous Mesoporous Mater.* **2003**, *62*, 81.
(10) Zheng, S.; Heydenrych, H. R.; Jentys, A.; Lercher, J. A. *J. Phys. Chem. B* **2002**, *106*, 9552.
(11) Weber, R. W.; Möller, K. P.; O'Connor, C. T. *Microporous Mesoporous Mater.* **2000**, *35–36*, 533.
(12) O'Connor, C. T.; Möller, K. P.; Manstein, H. *CATTECH* **2001**, *5*, 172.
(13) Duncan, W. L.; Möller, K. P. *Adsorption* **2005**, *11*, 259.
(14) Weidenthaler, C.; Wilczok, U.; Schmidt, W. X-ray Photoelectron Spectroscopy on Surface Modified MFI Zeolites. In *Proceedings of 18th German Zeolite Conference*; University of Hanover: Hanover, Germany, 2006; P42, p 191.
(15) Zheng, S.; Tanaka, H.; Jentys, A.; Lercher, J. A. *J. Phys. Chem. B* **2004**, *108*, 1337.
(16) Ban, T.; Brühwiler, D.; Calzaferri, G. *J. Phys. Chem. B* **2004**, *108*, 16348.
(17) Huber, S.; Calzaferri, G. *Angew. Chem., Int. Ed.* **2004**, *43*, 6738.
(18) Karge, H. G.; Niessen, W. *Catal. Today* **1991**, *8*, 451.
(19) Hermann, M.; Niessen, W.; Karge, H. G. *Stud. Surf. Sci. Catal.* **1995**, *94*, 131.
(20) Karge, H. G.; Niessen, W.; Bludau, H. *Appl. Catal., A* **1996**, *146*, 339.

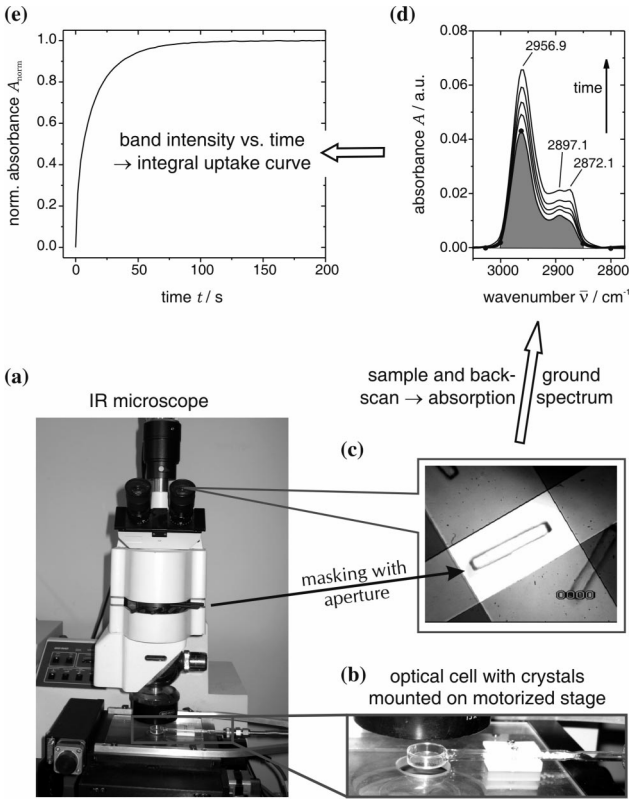

Figure 1. Schematic diagram of the infrared microscopy experimental technique. (a) IR microscope. (b) Optical cell with crystals inside. (c) Selected single crystal masked with aperture. (d) Band intensity monitored over a certain range of wavenumbers. (e) Uptake curve obtained by plotting band intensity at a specific wavenumber versus time.

The measurement of spectra and thus the local concentrations at different times allowed us to plot the overall uptake curve for the chosen crystal (Figure 1e). For the measurements, the C–H stretching vibration band of isobutane at around 2957 cm^{-1} was chosen. The integrals were calculated as area between 3000 and 2850 cm^{-1} enclosed by a straight baseline between the fixed anchor points at 3025 and 2800 cm^{-1} of the spectra. Further transformations of the spectra, such as baseline corrections, were not required. All spectra were measured with a spectral resolution of 16 cm^{-1}. The spectra were measured at regular time intervals (2–10 s). The overall schematic of the experimental setup is shown in Figure 1.

Samples. Our choice of zeolite type as samples for this study requires some explanation. Zeolites are crystalline aluminosilicates that have AlO_4^- and SiO_4 tetrahedra linked by oxygen bridges. One of the most commonly studied zeolite structure is that of the MFI-type. ZSM-5 and silicalite-1 are the most common MFI zeolites. The MFI structure is built by 5–1 secondary building units which are linked together to form chains. The chains, in turn, are interconnected to form a channel system (sinusoidal 10-ring channels of 5.1 × 5.5 Å and straight 10-ring channels of 5.3 × 5.6 Å). Silicalite-1 is an MFI-type structure whose framework contains only silicon and oxygen atoms. ZSM-5 has exactly the same structure, but some of the silicon is replaced by aluminum atoms. The presence of aluminum in the framework leads to a net negative charge that requires the presence of some cation to balance the charge. The Si/Al ratio is an important parameter that affects the adsorptive and diffusive properties of zeolites. As the ratio increases, the cation content decreases and the surface nature changes from hydrophilic to hydrophobic. Zeolites containing aluminum atoms can also be easily dealuminated with the corresponding loss of the crystalline structure by treatment with strong acids. We chose to use silicalite-1 crystals for our study because (1) their surface is electrically neutral, (2) there are no internal acid sites to influence the transport rates, and (3) they will not undergo dealumination upon treatment with acid solutions.

The silicalite-1 crystals used for the FTIR microscopy investigations were synthesized at the Max-Planck-Institute in Mülheim, Germany. The crystals were approximately 25 × 25 × 180 μm^3 in size. The unit cell parameters of the zeolite crystals are a = 20.07 Å, b = 19.74 Å, and c = 13.14 Å.[21] An optical picture of the crystal recorded by the CCD camera of the IR microscope is shown in Figure 1c.

Five different samples were selected for the experiments. One sample consisted of the parent crystals that had undergone only calcination. Another sample consisted of crystals that were surface treated with HF and then calcined. The remaining three samples were subjected to surface modification treatment. They were HF-etched, calcined, and then treated with three different trialkylchlorosilanes, $(CH_3)_3SiCl$, $(C_2H_5)_3SiCl$, and $(C_3H_7)_3SiCl$. The chemical vapor deposition technique was used for the first two trialkylchlorosilanes, and chemical liquid deposition was used for propylchlorosilane. The trialkylsilanes were anchored to silanol groups on the surfaces of the crystallites according to $\equiv Si–OH + R_3SiCl \rightarrow \equiv Si–O–SiR_3 + HCl$, with R = CH_3, C_2H_5, or C_3H_7. Preliminary results on characterizing these samples by X-ray photoelectron spectroscopy have been reported recently.[14]

Sample Preparation. For activation, about 1000 crystals were introduced into the IR cell and heated under vacuum ($<10^{-5}$ mbar) with a heating rate of 1 K min^{-1}. The activation temperature for the silanated samples was set to 363 K and to 753 K for the HF treated and calcined samples. The activation temperature for the silanated samples was limited to 363 K to prevent the occurrence of coking of the surface layer. The crystals were left at the elevated temperature for 24 h. Then the crystals were cooled to 298 K, and the sorption experiment was started after selecting one crystal for the measurement. Adsorption and desorption experiments were performed with isobutane. Several runs were performed between the pressure steps of vacuum and 1 mbar and vacuum and 10 mbar. In addition, experiments were also performed with crystals subjected to differential pressure changes in the Henry's law region.

Data Analysis

All the adsorption and desorption rate data were fitted to the solution of diffusion equation with an assumed constant integral diffusivity (D) between the two loadings corresponding to the initial and final pressures. The solution of differential equation used to describe uptake in a three-dimensional channel network in infinitely long cylindrically shaped particles with the assumption of equilibrium at the boundary between the gas and adsorbed phase (no surface resistance) is represented by[22]

$$A_{\text{norm}} \equiv \frac{A_t - A_0}{A_\infty - A_0} = 1 - 4\sum_{n=1}^{\infty} \frac{1}{a_n} \exp\left(-\frac{a_n D t}{r_{\text{cyl}}}\right) \quad \text{with} \quad J_0(a_n) = 0 \quad (1)$$

Here J_0 is the zeroth-order Bessel function of the first kind and A_0, A_t, and A_∞ describe the absorbance at time 0, t, and ∞, respectively. Consequently, the normalized absorbance

(21) Baerlocher, Ch.; McCusker, L. B. Database of Zeolite Structures: http://www.iza-structure.org/databases/.
(22) Crank, J. *Mathematics of Diffusion*, 2nd ed.; Oxford University Press: New York, 1975.

Table 1. Parameters Obtained from Fitting the Experimental Data Using Eq 1 for Diffusion Control and Eq 2 for the Combined Influence of Diffusion and Surface Resistances

		diffusion model		dual resistance			
		$D/10^{-13}$ m^2 s^{-1}		$D/10^{-13}$ m^2 s^{-1}		$\alpha/10^{-7}$ m s^{-1}	
material	step/ mbar	ads	des	ads	des	ads	des
HF-etched	0–1	13.6	5.04	13.6	5.04		
	0–10	22.2	5.10	22.2	5.10		
calcined	0–1	13.7	5.78	13.7	5.78		
	0–10	22.9	5.65	22.9	5.65		
$(CH_3)_3SiCl$	0–1	1.87	1.06	13.7	5.41	0.79	0.47
(crystal 2)	0–1	1.18	0.31	13.7	5.41	0.40	0.10
	0–10	3.28	1.00	22.6	5.38	1.39	0.44
$(C_2H_5)_3SiCl$	0–10	0.77	0.17	22.6	5.38	0.23	0.05
n-butane in $(C_3H_7)_3SiCl$	0–30	0.04					

A_{norm} as defined in eq 1 corresponds to the fractional uptake at time t.

If the surface barrier/resistance is present at the boundary, then the concentrations in the gas phase and at the crystal boundary are not in equilibrium, and the flux across the crystal boundary is given by $\alpha(C_e - C)$. Here α is the surface permeability, C_e is the adsorbed phase concentration in equilibrium with the prevailing pressure in the optical cell, and C is the adsorbed phase concentration at the edge of the crystal. A larger value of surface permeability signifies a lower magnitude of surface resistance and vice versa. The solution of diffusion into cylindrical geometry with surface resistance is given by[22]

$$A_{\text{norm}} = 1 - \sum_{n=1}^{\infty} \frac{4L^2 \exp(-\beta_n^2 Dt/r_{\text{cyl}}^2)}{\beta_n^2(\beta_n^2 + L^2)}$$

$$\text{with} \quad \beta_n J_1(\beta_n) - L J_0(\beta_n) = 0 \text{ and } L \equiv \frac{\alpha r_{\text{cyl}}}{D} \quad (2)$$

Here J_0 and J_1 are the zeroth- and first-order Bessel functions of the first kind. The equivalent radius of the crystal was calculated using $r_{\text{cyl}} = wh/(w + h)$ with w and h representing the crystal dimensions in x and y directions. The first 100 terms were used for the curve fitting for given values of parameters α and D. The results from curve fitting for all runs are summarized in Table 1.

Results and Discussion

Effect of Loading on Rates of Adsorption and Desorption. *Large Pressure Change.* The adsorption and desorption runs for pressure change between vacuum and 10 mbar for untreated samples are shown in Figure 2. Figure 2a shows the uptake curves for adsorption, and Figure 2b shows the results for desorption. The results are plotted in terms of integrated areas under the characteristic bands which is proportional to the average local concentration. The figures show results for four consecutive cycles of adsorption and desorption experiments performed on the same crystal. The results show excellent reproducibility as the experimental data for all four runs lie essentially on top of one another.

Another important aspect evident from the data is that desorption is slower than adsorption as indicated by the time to complete the runs (about 100 s for adsorption versus 400 s for desorption). We fitted the adsorption and desorption curves to eq 1. In doing so, we assumed that for these untreated samples no surface barrier was present and only intracrystalline diffusional resistance was present in this case. The rationale for not considering surface resistance for the untreated samples is given little later while discussing Figure 6. The corresponding effective diffusivities calculated from eq 1 for adsorption and desorption steps are 22.9×10^{-13} and 5.7×10^{-13} m^2 s^{-1}. The effective intracrystalline diffusivity is higher by a factor of 4 for the adsorption step than it is for the desorption step. This observation is the result of significant variation of intracrystalline diffusivity with adsorbate loading in the crystal. The imposed pressure change (between 0 and 10 mbar) is large enough to substantially change the loading between the initial and final pressures. If the intracrystalline diffusivity increases with loading, then as the loading in the crystal increases, the diffusivity and hence the rate of adsorption also increase. However, during desorption, the loading decreases with time, resulting in lower diffusivity. As a result, the rate of desorption decreases and is much slower than the rate of adsorption. For the methanol–ferrierite system, we have demonstrated that the huge differences between the transient concentration profiles for uptake and release are explained by the concentration dependence of transport diffusivities.[23]

Adsorption Isotherm and Thermodynamic Correction Factor. To get a better understanding of how the intracrystalline loading at equilibrium changes with pressure, single crystal sorption isotherm was recorded for three different crystals using IR microscopy. The gas phase pressure of isobutane was increased stepwise between 0 and 10 mbar. For each of the small pressure steps, the corresponding absorbance was measured after equilibrium was established and plotted against pressure (see Figure 3). The isotherms were scaled to follow the data of crystal 1. Small differences in the size of crystals originally produced small deviations between the values of integral concentration. However, after these size differences were accounted for, all isotherms showed excellent agreement. As far as we know, this is the first investigation where the adsorption isotherms of different individual crystals of one batch have been measured and compared.

The measured isotherm was compared with the literature data in the temperature range 300–310 K. Most isotherms were measured at a slightly higher temperature and showed the expected shift to higher pressures. Nearly perfect agreement was found with the CBMC simulation results at temperature of 298 K.[24] The simulation results could be well described a dual-site Langmuir model. The correlation of the IR data and the simulation results allowed us to calculate the corresponding equilibrium concentration for each pressure in the considered range.

(23) Kortunov, P.; Heinke, L.; Vasenkov, S.; Chmelik, C.; Shah, D. B.; Kärger, J.; Rakoczy, R. A.; Traa, Y.; Weitkamp, J. *J. Phys. Chem. B* **2006**, *110*, 23821.

(24) Chmelik, C.; Heinke, L.; Kärger, J.; Schmidt, W.; Shah, D. B.; van Baten, J. M.; Krishna, R. Inflection behavior in the loading dependence of the Maxwell-Stefan diffusivity of iso-butane in MFI zeolite investigated by Infra-Red Microscopy and Kinetic Monte Carlo Simulations. *Chem. Phys. Lett.* **2007**, in press.

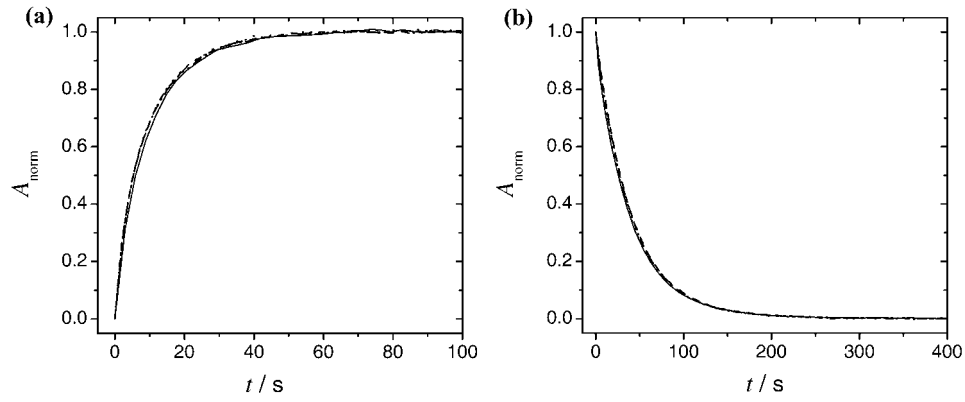

Figure 2. Relative uptake/release during pressure change between 0 and 10 mbar: (a) is for adsorption and (b) is for desorption.

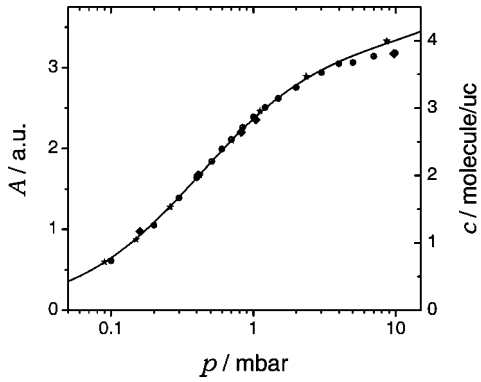

Figure 3. Adsorption isotherm of isobutene on untreated samples using IR microscopy: crystal 1 (●), crystal 2 (▲), and crystal 3 (★). The full line represents calculated values from CMBC simulations.[24]

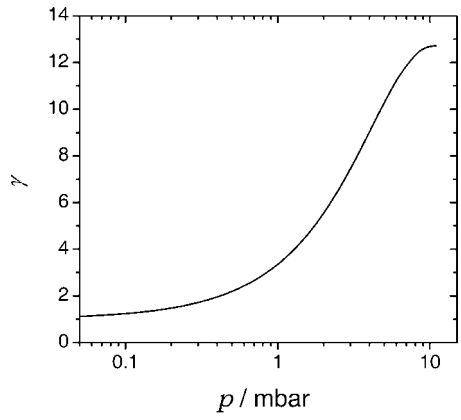

Figure 4. Thermodynamic correction factor for isobutane on untreated samples calculated from the isotherm data in Figure 3.

The transport diffusivity (D) and the corrected diffusivity (D_0) are related to one another by the thermodynamic correction factor γ as given by

$$D = D_0\gamma = D_0 \frac{\mathrm{d}\ln(p)}{\mathrm{d}\ln(c)} \tag{3}$$

The thermodynamic factor has the value of 1 in the Henry's law region and increases exponentially as the isotherm shape flattens. Its value, for the present system, was calculated by numerical differentiation of the adsorption isotherm and is shown as a function of pressure in Figure 4. As expected, the correction factor is a strong function of pressure and increases from 1 in the Henry's law region to 12.7 at a pressure of 10 mbar. Implying that this dependence is not compensated by the concentration dependence of D_0, hence the integral transport diffusivity calculated from uptake and release curves for pressure steps between 0 and 10 mbar will be significantly different from the differential diffusivity and corrected diffusivity calculated at a specific loading. Our previous work has conclusively shown that variation of transport diffusivity with loading is mainly responsible for differences in rates of adsorption and desorption.[23] Only in the linear region of the isotherm or for differential pressure steps is the transport diffusivity constant, and the theory predicts the adsorption and desorption curves to be mirror images of one another.

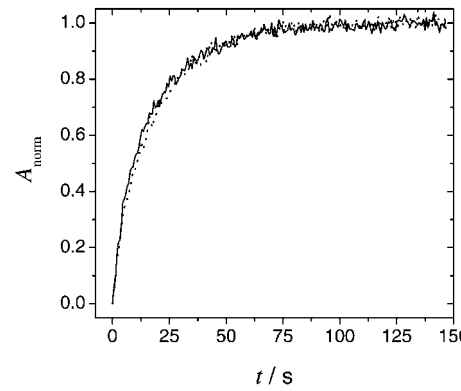

Figure 5. Adsorption (—) and desorption (···) curves for differential pressure steps.

Differential Pressure Change. To substantiate this argument, we performed adsorption and desorption runs on HF-etched samples in the Henry's law region where the isotherm is practically linear and the thermodynamic correction factor is close to 1. Figure 5 shows the adsorption and desorption runs in the Henry's law region with differential pressure steps between 0.05 and 0.1 mbar. The estimated loading at 0.05 mbar is 0.43 molecule/uc and that at 0.1 mbar is 0.78 molecule/uc. Here the "uc" refers to unit cell. The thermodynamic correction factors at these pressures are 1.12 and 1.24, respectively, indicating that the adsorption isotherm in this pressure range is essentially linear. The desorption run is plotted in terms of A_{norm} rather than $1 - A_{norm}$ to compare the two shapes. The two curves are identical, indicating that for differential steps the adsorption and desorption curves are symmetrical. For integral steps, as depicted in Figure 2, the adsorption and desorption curves are asymmetrical.

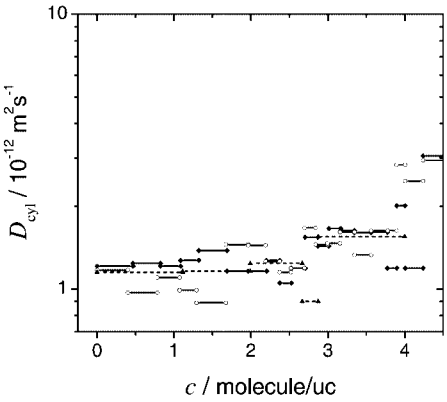

Figure 6. Transport diffusivity of isobutane as a function of loading for the calcined (♦–♦ for crystal 1 and ▲–▲ for crystal 2) and HF-treated samples (○–○).

Transport Diffusivity as a Function of Loading. The kinetics of uptake of isobutane in calcined and HF-etched crystals was also measured over several differential pressure steps in the range of 0–20 mbar. Equation 1 was used to calculate the transport diffusivity. Since the imposed pressure changes were differential, the assumption of constant transport diffusivity is justified. The calculated transport diffusivity as a function of loading is shown in Figure 6. This figure exhibits several features. It shows that the transport diffusivity does increase significantly (by a factor of 2.5) as the loading increases to 4 molecule/uc. This is consistent with what has been observed in Figure 2 and Figures 7 and 8. Second, the figure shows remarkable reproducibility of the results when measurements were performed on two different calcined crystals from the same batch. Finally, the figure shows the same loading dependence of transport diffusivity for HF-etched and calcined crystals. This shows that the magnitude of the surface barrier associated with both these crystals is about the same. HF etching did not have an effect on the surface permeability of the silicalite-1 crystals.

Effect of Surface Treatment. Figures 7 and 8 show the comparison of adsorption and desorption curves for samples with different surface treatments. The pressure steps were between 0 and 1 mbar for Figures 7a and 8a and between 0 and 10 mbar for Figures 7b and 8b. These figures exhibit several important features.

The uptake/release curves for the untreated and the HF-etched crystals are steep and quite rapid. Since the HF-etched crystals would be expected to show the least surface resistance, it was assumed that HF-etched crystals would not exhibit any surface barrier. Since the response curves for untreated (but calcined) crystals lay on top of those for the HF-etched crystals, we also assumed that the untreated crystals also did not exhibit any surface barrier. Thus, the experimental response curves were fitted to eq 1 to determine the effective intracrystalline diffusivities. These are termed effective diffusivities because we know that the diffusivity depends on concentration for this step. The thermodynamic factor at low pressure is 1, and that at 1 mbar is 3.4. Moreover, both eq 1 and eq 2 imply a constant diffusivity. The diffusivity values for the untreated samples were determined to be 13.7×10^{-13} and 5.8×10^{-13} m^2 s^{-1} for adsorption and desorption steps, respectively, for the pressure step between 0 and 1 mbar.

The values for the same samples for the larger pressure step are 22.9×10^{-13} and 5.7×10^{-13} m^2 s^{-1} for the adsorption and desorption pressure steps. The values for the adsorption step for the larger pressure change is greater than the one for the lower pressure step (22.9 versus 13.7) as would be expected for the case of increasing diffusivity with increasing concentration.

The HF-etched samples essentially behaved similarly to the untreated samples with no surface barriers. This is contrary to what has been reported in the literature.[7,9] However, in both previous references cited, the HF-etching was performed on ZSM-5 samples whereas silicalite-1 crystals were used in the present study. HF-etching of ZSM-5 crystals likely produces dealumination which may be responsible for the observed reduction of surface barrier. However, because of the absence of aluminum in silicalite-1, no such surface barrier reduction is observable.

The uptake/release curves are slower for the crystals modified with trimethylchlorosilane than the untreated or HF-treated crystals and are the slowest for the sample modified with triethylchlorosilane. The response curves for samples treated with tripropylchlorosilane are not shown because no visible uptake was observed. The experiments were repeated with other crystals of the same sample, but a very slow or no uptake was observed. The pores appeared to be completely blocked by the $(C_3H_7)_3Si$– when the crystals were silanized with tripropylchlorosilane. This surface treatment was achieved by the chemical liquid deposition technique whereas zeolite samples were modified with trimethyl- and triethylchlorosilanes using chemical vapor deposition. It is not clear at this point whether the different method of preparation used was responsible for the complete pore blockage. We also attempted to measure the uptake rate of a smaller molecule such as *n*-butane for a much larger pressure step (0–30 mbar). *n*-Butane diffusion in MFI crystals should be much more rapid considering the size of the pore window (5.5 Å) and the size of the diffusing molecule (4.3 Å), in comparison to isobutane (5.0 Å). The uptake was extremely slow for samples treated with tripropylchlorosilane. The effective diffusivity of *n*-butane calculated from the response curve was 4×10^{-15} m^2 s^{-1}. This value is lower by a factor of 550 from the ones calculated for isobutane diffusion in untreated samples. An approximate calculation showed that the ratio of *n*-butane diffusivity in untreated sample and that in sample treated with tripropylchlorosilane is of the order of 10^5. The treatment with tripropylchlorosilane appears to significantly reduce the effective pore size as indicated by the significantly reduced uptake rate of *n*-butane. The uptake/release rates decrease significantly due to surface treatment with different trialkylchlorosilanes. Surface modification, therefore, does increase the magnitude of the surface resistance, and this magnitude increases with the increasing size of the alkyl groups.

One and Two Resistance Models. The decreasing rates of uptake/release curves were interpreted in two different ways. First, it was assumed that even though two separate resistances existed in the diffusion process (surface barrier

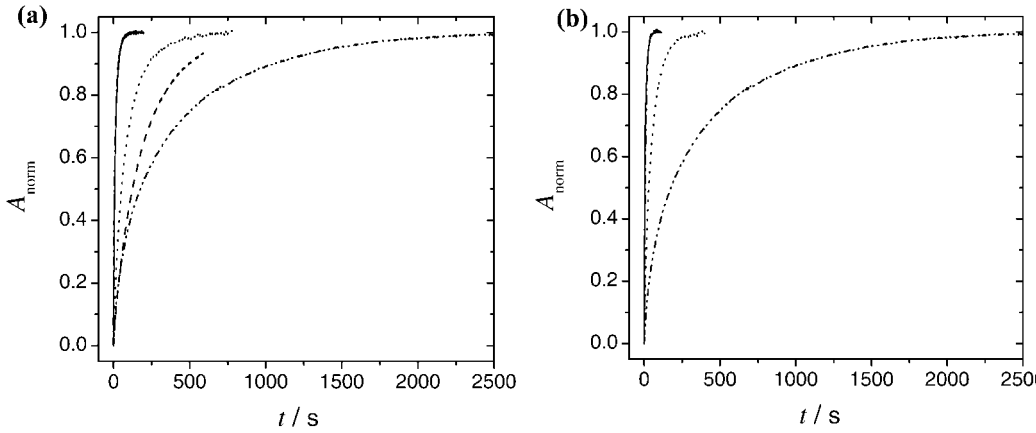

Figure 7. Comparison of adsorption curves for samples with different surface treatments: HF-etched (-•-), calcined (—), –$Si(CH_3)_3$ (••• for crystal 1 and --- for crystal 2), and –$Si(C_2H_5)_3$ (-••-). The pressure steps were between 0 and 1 mbar for (a) and 0 and 10 mbar for (b).

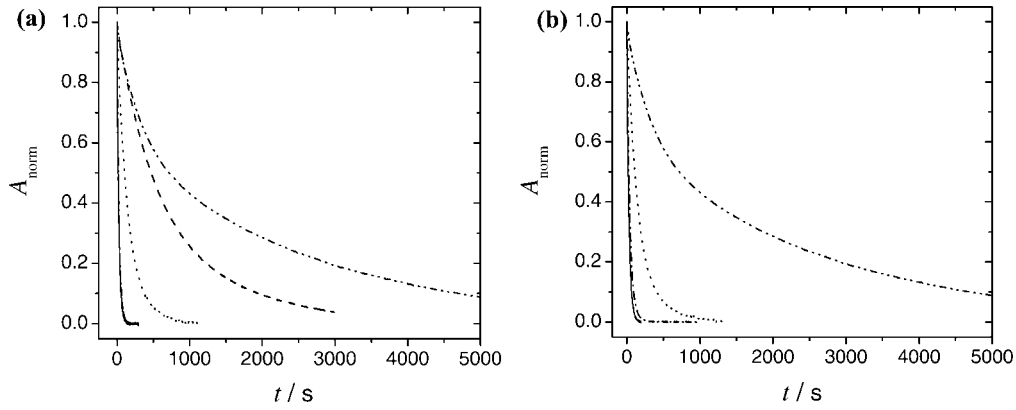

Figure 8. Comparison of desorption curves measured for crystals with different surface treatments: HF-etched (-•-), calcined (—), –$Si(CH_3)_3$ (••• for crystal 1 and --- for crystal 2), and –$Si(C_2H_5)_3$ (-••-). The pressure steps were between 1 and 0 mbar for (a) and 10 and 0 mbar for (b).

followed by intracrystalline diffusion), the process can be modeled as a lumped parameter system with one resistance characterized by an effective diffusion coefficient. Another way of modeling the system involves using a distributed parameter model with two distinct resistances: surface barrier and the intracrystalline diffusional resistance.

Lumped Parameter Model. The uptake/release curves were fitted to eq 1, and the effective diffusivities were calculated. The effective diffusivity parameter will be dependent on the magnitudes of the individual resistance. The determined values are listed in Table 1. The effective diffusivities for trimethylchlorosilane-treated samples are of the order of (1–3) $\times$ 10^{-13} m^2 s^{-1} for adsorption and about (0.5–1) $\times$ 10^{-13} m^2 s^{-1} for desorption. The adsorption step diffusivities are lower by an order of magnitude, whereas the desorption diffusivities are lower by a factor of about 5 compared to the values of the untreated sample. For samples treated with triethylchlorosilane, the adsorption and desorption diffusivities are about 0.77 $\times$ 10^{-13} and 0.17 $\times$ 10^{-13} m^2 s^{-1}. In this case, the adsorption and desorption diffusivities are lower than those for untreated samples by a factor of about 30. The effective diffusivities have therefore decreased substantially with surface treatment, and as the size of the alkyl group used in the chlorosilane increases, the surface barrier tends to increase, thereby reducing the magnitude of the effective diffusivity. In every case, the desorption diffusivity is lower than the adsorption diffusivities as expected.

Distributed Parameter Model. In this model, both surface barrier and intracrystalline diffusional resistances (characterized by parameters α and D) are accounted for. Equation 2 is used for calculating the uptake/release curves. In this analysis, we assumed that the surface treatment only changes the effective diameter of the window, thereby changing the magnitude of the surface resistance. However, once the diffusing molecule overcomes this barrier, the diffusion process would be characterized by the same intracrystalline diffusivity that was determined for the untreated samples. Hence, eq 2 was used with the same values of D as were determined for untreated crystals. The best values of parameter α determined under the above constraint are shown in the table in the last two columns. The values of α for samples treated with trimethylchlorosilane are in the range about 1 $\times$ 10^{-7} m s^{-1}, and that for the sample treated with triethylchlorosilane is 0.23 $\times$ 10^{-7} m s^{-1}, 1/4th of the previous value. Thus, the surface permeability of samples treated with triethylchlorosilane is lower by a factor of 4 than the values for the samples treated with trimethylchlorosilane. Its surface resistance is, therefore, correspondingly that much larger.

In Figure 7a, uptake curves for two different crystals from the same sample that was treated with trimethylchlorosilane are shown. The uptake curves are sufficiently different for the two crystals. Both these crystals, thus, exhibit different surface resistances even though they were obtained from the

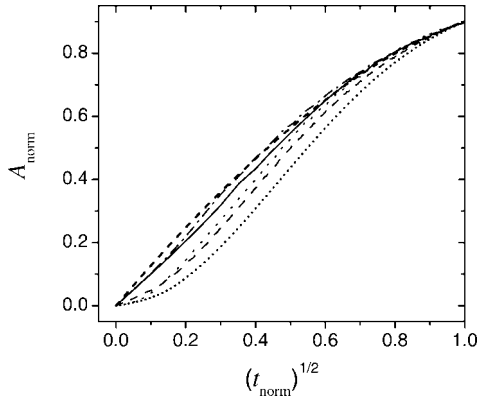

Figure 9. Uptake plotted versus square root of normalized time for 0–1 mbar curves for different samples: HF-etched (-•-), calcined (—), and $(CH_3)_3SiCl$ (••• for crystal 1 and --- for crystal 2). The curves were normalized in time to allow a direct comparison. The shape changes most distinctively from diffusion control (---) for the HF-etched and untreated samples to barrier limitation (•••) for the surface-silanated samples.

same batch. It is clear that we need to improve our surface treatment methods in order to produce consistent surface resistance for all crystals throughout the sample.

The ability to track the kinetics of adsorption/desorption on a single crystal is an important feature of the IR microscopy technique. Most other techniques measure overall uptake/release rates for an aggregate of crystals. Measurements on individual crystals can determine whether adsorptive and diffusive properties of individual crystals are similar or different and thus whether the synthesis method produces uniform-quality crystals throughout the batch.

In Figure 9, the uptake/release rates are plotted against the square root of time for 0–1 mbar curves. All curves are normalized in time with respect to the time needed to reach $A_{norm} = 0.9$ to compare their shapes. For diffusion-controlled processes, one expects to see initial straight line whereas for surface-barrier-controlled processes, one expects to see an S-shaped curve. The curve corresponding to surface-barrier limitation has the highest degree of S-shape. The responses associated with untreated or HF-treated samples show straight lines near origin, indicating purely diffusion control and complete absence of surface resistance. As the magnitude of surface barrier increases, one should expect to see an increasing degree of S-shaped responses. The figure only shows the response curve for samples treated with trimethylchlorosilane. It does show a distinct S-shaped character. However, the curve for samples treated with triethylchlorosilane lies quite close to that for the sample treated with trimethylchlorosilane. Hence, that curve is not shown. Of course, the tripropylchlorosilane-treated sample showed no isobutane uptake anyway. The presence of S-shaped nature of the response curves clearly indicates presence of a surface barrier for the trimethylchlorosilane-treated sample. The uptake curves shown in Figures 7 and 8 indicate a greater magnitude of the surface resistances for triethylchlorosilane-treated sample. The results indicate that the magnitude of the surface resistance increases with the size of the alkyl groups used in chlorosilanes to modify the zeolite surface in the order trimethyl- < triethyl- < tripropylchlorosilane.

Variation of α *with Loading.* It is important to emphasize that the values of α determined for adsorption and desorption steps for the same pressure step are different. For example, for samples treated with trimethylchlorosilane, the values of α for adsorption and desorption for 0–1 mbar pressure step were 0.4 and 0.1 m s^{-1}, respectively, whereas those for the 0–10 mbar pressure step were 1.39 and 0.44 m s^{-1}, respectively. In both cases, the desorption values are lower by a factor of 3–4. For samples treated with triethylchlorosilane, both α values are lower than those for samples treated with trimethylchlorosilane, but the value for adsorption is still about a factor of 4 higher than that for desorption (0.23 versus 0.05). The different values of α for adsorption and desorption signifies that α, just like the transport diffusivity, is also dependent on loading. The surface barrier is greater for the case of desorption than that for adsorption for the same pressure step.

It is important to recognize that the infrared microscopy method used here is a mesoscopic/ macroscopic method and therefore provides no direct evidence of the nature of the surface barrier. The surface barrier formed due to the surface treatment could arise simply from a surface-related phenomenon such as the reduction of the effective pore diameter due to the presence of a large organic molecule near the pore window. It could also arise from the internal molecule–molecule or adsorbent–adsorbate interactions in the pore. It is very likely that both these factors determine the nature of the surface barrier. They also could explain the dependence of α on loading/concentration.

Conclusions

Surface silanization works as a method to produce surface barriers of different strengths. The rates of diffusion into and out of the crystals correlated well with the strength of the surface barrier. The untreated and HF-treated samples appeared to have the fastest uptake/release rates: however, the samples treated with trimethylchlorosilane exhibited slower overall uptake rates, and those treated with triethylchlorosilane showed the slowest uptake. The sample treated with tripropylchlorosilane revealed very slow or no uptake, indicating a nearly complete pore blockage. Crystals from the same batch exhibited different surface resistances indicating the need to improve the surface modification methods to produce crystals with uniform surface barriers. Such surface modification procedures will be useful for detailed fundamental study as well as tailoring zeolites for specific applications.

Acknowledgment. Financial support by Deutsche Forschungsgemeinschaft (Gast-Mercator award to DBS, International Research Group "Diffusion in Zeolites" and International Research Training Group "Diffusion in Porous Materials"), Max-Buchner-Forschungsstiftung, and Fonds der Chemischen Industrie is gratefully acknowledged.

CM071632O